h.$^{-1}$ The exchanges of the Glu(A17) and Ala(B14) amide protons are somewhat slower, but are still too fast to allow the cross peaks to be observed under the applied experimental conditions.

As discussed above, the internal consistency of the exchange rates determined by the method is demonstrated by the close agreement between the rates obtained from different cross peaks that are influenced by the same exchange process. Also, the reproducibility of the method is evidenced by the accordance between the two experiments in Table I. Still, the compatibility of the rates determined by the method described here and by classical methods[1-3] remains to be established. To that end, the exchange rates of the amide protons of the Val(B18) and Gln(A15) residues, both of which have NH signals with no or little overlap (cf. Figure 1), were determined by monitoring the decays of the two NH signals in a series of 1D spectra recorded immediately after dissolution of the des-[Phe(B25)] insulin in D_2O. The experiment was carried out at pH 3.5 and 310 K, using a 5 mM solution. Although this pH value was slightly higher than the pH value (3.0) of the sample used in the 2D experiment, both values are close to the pH that corresponds to the minimum of the exchange rate of peptide-group hydrogens.[24] Accordingly, the NH exchange rates of 0.234 ± 0.003 and 2.27 ± 0.03 h^{-1}, obtained for Val(B18) and Gln(A15), respectively, from the series of 1D spectra, are both in close agreement with the values obtained in the 2D experiment (cf. Table I). The fact that the 1D value in the case of Val(B18) is the same as the corresponding 2D value within the uncertainty, while it is about a factor of 2 larger in the case of Gln(A15), shows that the pH value for the minimum of the exchange rate of the Gln(A15) NH is lower than that of Val(B18). According to the rules of Molday et al.,[24] this difference in minima is in qualitative agreement with the difference in the primary structure around the two residues.

Finally it should be noted that the range covered by the proposed method can be expanded to include exchange rates slower than those determined here, by increasing the time of the experiment through an increase of the number of scans per t_1 value, or by increasing the sweep width in the F_1 dimension. Thus, for a given R_2^* rate and a given number of experimental data points in the t_1 dimension, an increase of the F_1 sweep width decreases the relaxation decay monitored during a given experimental time, whereas the decay of the FID caused by the exchange remains unaffected. Consequently, for a given relaxation rate, slower exchange processes will affect the FID and can be monitored.

Conclusion

It has been demonstrated that the method presented here allows a quantitative determination of amide proton exchange rates of the order of reciprocal hours. Designing the experimental conditions to the expected exchange rates makes it possible to cover a wider range of rates. Thus the upper limit for the exchange rates covered by the method can be raised by reducing the time of the experiment as demonstrated here, and a combination of this method with the method[5] for fast recording of 2D NMR spectra could possibly extend the range to cover exchange rates of the order of reciprocal minutes. The lower limit for the exchange rates covered by the method is given by the R_2^* relaxation rate and the sweep width in the F_1 dimension and can, in principle, be regulated by adjusting the sweep width.

The applied linear prediction program, LPEXTRAPOL, which is capable of handling TPPI data, and the applied LSQ program, NMRFIT, both written in VAX/VMS FORTRAN, can be obtained from the authors by request.

Acknowledgment. This work was supported by the Danish Technical Research Council, J. No. 16-4679.H, the Danish Natural Science Research Council, J. No. 11-8977-1 and 16-5027, the Ministry of Industry, J. No. 85886, Direktør Ib Henriksens Fond, and Julie Damms Studiefond. We also thank Dr. Per Balschmidt Novo Nordisk A/S for providing the des-[Phe(B25)] insulin.

---

[24] Molday, R. S.; Engelander, S. W.; Kallen, R. G. *Biochemistry* **1972**, *11*, 150–158.

Conformational Analysis of Six-Membered Rings in Solution: Ring Puckering Coordinates Derived from Vicinal NMR Proton–Proton Coupling Constants

C. A. G. Haasnoot

Contribution from the Department of Analytical Chemistry, Scientific Development Group, Organon International B.V., P.O. Box 20, 5340 BH Oss, The Netherlands.

Received July 20, 1992

Abstract: A new method for quantitative analysis of the conformation of six-membered ring compounds in solution is presented. The method uses as a probe the endocyclic vicinal NMR proton–proton coupling constants, which are translated into the relevant conformational parameters by means of a combination of the generalized Karplus equation and the recently developed Truncated Fourier formalism (delineating the interrelation between the endocyclic torsion angles in a six-membered ring; cf.: Haasnoot, C. A. G. *J. Am. Chem. Soc.* **1992**, *114*, 882). A practical elaboration is laid down in three computational procedures which can be used to analyze the experimental couplings in terms of a single-state conformation or a two-state conformational equilibrium. Typical applications of these procedures are exemplified by conformational analyses of six-membered rings occurring in alkaloids, steroids, and sugar derivatives. The obtained conformational descriptions of these six-membered rings in solution are shown to be consistent with conformational data derived from X-ray crystallography and/or molecular mechanics. It is, therefore, concluded that the unique quantitativeness of the method allows for a superior analysis of the conformational behavior of six-membered rings in solution.

Introduction

Nuclear magnetic resonance (NMR) plays an important role in the conformational analysis of (bio-)(macro-)molecules in solution. One of the pillars of its success is the widespread application of proton–proton coupling constants to conformational problems. A long-standing and rather straightforward example of such an application in the field of six-membered ring systems is the determination of the equilibrium between rapidly exchanging

0002-7863/93/1515-1460$04.00/0

(chair) conformers.[1] In this case the observed coupling constants are time-averaged,[2] i.e.

$$J_{\text{obs}} = \sum_i \alpha_i J_i \tag{1}$$

where J_i are the values of the limiting coupling constants in a particular conformation i with molar fraction α_i. Once a set of limiting J_i values is assumed, e.g., on the basis of rigidized model compounds, and a sufficient set of experimental couplings is known, eq 1 allows the calculation of the α_i values involved[1] and hence the free energy differences between the corresponding conformers. There exists an uncounted number of published investigations of this type which contributed to useful conceptual abstractions as "conformational energies" or "*A* values",[3] etc.

Another application of coupling constants in six-membered rings is to determine the ring conformations. Typically, this is done by translating experimental vicinal proton–proton couplings into H–H torsion angle information using Karplus-type relations.[4] Supposing that the protons are located on the six-membered ring, this information can then provide the endocyclic torsion angles needed for the description of the ring conformation. Although in principle straightforward, in practice the latter approach is hampered by the limited accuracy of both the experimental couplings and (especially) the Karplus relation used. The propagated errors are usually too large to yield precise information on the individual endocyclic torsions,[5] and therefore this approach is commonly used only in a qualitative way to classify six-membered rings in terms of chairs, boats, half-chairs, etc.[6]

In the past, several attempts have been made to obtain more (in the sense of: better) quantitative information on the six-membered ring conformation from vicinal coupling constants. Notable examples of such attempts are the so-called *R*-value method[7,8] and variations on that theme.[9,10] However, the theoretical foundation as well as the applicability of these methods is rather limited. Moreover, at their best such methods yield information on single endocyclic torsions only. As such, they do not lead to an integrated and consistent quantitative picture of the six-membered ring conformations involved.

In this paper a new method is presented which resolves the difficulties mentioned above by explicitly taking the interrelation[11] between the endocyclic torsions in a six-membered ring into account. This diminishes the influence of random errors in experimental couplings and the limited accuracy of the (generalized) Karplus equation[12] considerably. Moreover, it will be shown that this new method can also be used in situations where the six-membered ring is involved in a conformational equilibrium. In the latter case the method combines the two types of applications of coupling constants described above. In all circumstances a superior analysis of the conformational aspects of six-membered rings in solution is obtained.

Procedures

The conformational analysis of six-membered rings is facilitated by the Truncated Fourier (TF) formalism[11] which describes the interdependence of the endocyclic torsions (ϕ_j, $j = 0, 1, ..., 5$; cf. Figure 1) in the ring, viz.

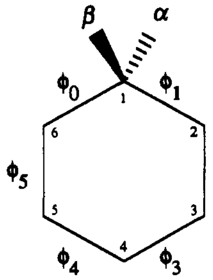

Figure 1. Atom and torsion angle numbering in six-membered rings. Since the values of the puckering coordinates (P_2, Φ_2, and Φ_3 in eq 2) depend on the choice of the origin torsion angle ϕ_0, the following numbering scheme is adopted for purposes of eq 2: ring atom 1 is the atom with the lowest number according to IUPAC rules (e.g., the heteroatom in heterocycles; see also Boeyens[13] for useful extensions). The rest of the ring atoms are numbered 2 to 6 in clockwise order, working from any accepted standard or well-defined projection of the molecule. The endocyclic torsion about the bond between atom 6 and atom 1 is defined as ϕ_0, the torsion about the bond between atom 1 and atom 2 as ϕ_1, and so forth. Note that the so-called α- and β-positions on the ring skeleton correspond to "bottomside" (i.e., under the plane of projection) and "topside" (i.e., above the plane of projection) locations of substituents, respectively.

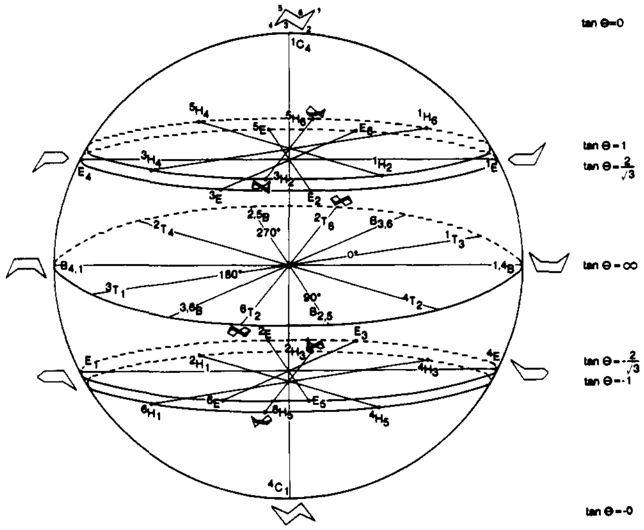

Figure 2. Schematical representation of the sphere on which the conformations of six-membered rings can be mapped (for a constant value of Q). Canonical conformations are indicated (C = chair, E = envelope or sofa, H = half-chair, B = boat, T = twist-boat).

$$\phi_j = \Phi_2 \cos(P_2 + 4\pi j/6) + \Phi_3 \cos(\pi j) \tag{2}$$

The puckering coordinates Φ_2, P_2, and Φ_3 define the conformation of a given six-membered ring as a single point in a cylindrical conformational space. This conformational space contains one pseudorotational subspace of dimension two (Φ_2 and P_2, first right-hand-side term in eq 2) and one inversional subspace of dimension one (Φ_3, second right-hand-side term in eq 2). The pseudorotational subspace corresponds to the boat/twist-boat itinerary as given by Buys and Geise,[14] whereas the inversional subspace delineates the undistorted chair as defined by Bucourt.[15] Hence, every six-membered ring conformation may be viewed as a linear combination of the basis forms, i.e., boat, twist-boat, and chair. Note that the puckering coordinates (Φ_2, P_2, Φ_3) may be

---

(1) See, e.g.: (a) Jackman, L. M.; Sternhell, S. Applications of Nuclear Magnetic Resonance Spectroscopy in Organic Chemistry. *International Series of Monographs in Organic Chemistry*; Barton, D. H. R., Doering, W., Eds.; Pergamon Press: Oxford, 1969; Vol. 5. (b) Lambert, J. B.; Shurvell, H. F.; Verbit, L.; Cooks, R. G.; Stout, G. H. *Organic Structural Analysis*; Macmillan: New York, 1976.

(2) Pople, J. A. *Mol. Phys.* **1958**, *1*, 3.

(3) (a) Winstein, S.; Holness, N. J. *J. Am. Chem. Soc.* **1955**, *77*, 5562. (b) Hirsch, J. A. *Topics in Stereochemistry*; Eliel, E. L., Allinger, N. L., Eds.; Interscience: New York, 1967; Vol. 1, p 199. (c) Jensen, F. R.; Bushweller, C. H. *Adv. Alicycl. Chem.* **1971**, *3*, 139.

(4) Karplus, M. *J. Chem. Phys.* **1959**, *30*, 11.

(5) Cazaux, L.; Navech, J. *Org. Magn. Reson.* **1975**, *7*, 26.

(6) See, e.g.: Castellino, S.; Leo, G. C.; Sammons, R. D.; Sikorski, J. A. *J. Org. Chem.* **1991**, *56*, 5176.

(7) Lambert, J. B. *J. Am. Chem. Soc.* **1967**, *89*, 1836.

(8) Buys, H. R. *Recl. Trav. Chim. Pays-Bas* **1969**, *88*, 1003.

(9) Slessor, K. N.; Tracey, A. S. *Can. J. Chem.* **1971**, *49*, 2874.

(10) Lambert, J. B.; Sun, H.-n. *Org. Magn. Reson.* **1977**, *9*, 621.

(11) Haasnoot, C. A. G. *J. Am. Chem. Soc.* **1992**, *114*, 882.

(12) Haasnoot, C. A. G.; Leeuw, F. A. A. M. de; Altona, C. *Tetrahedron* **1980**, *36*, 2783.

(13) Boeyens, J. C. A. *J. Cryst. Mol. Struct.* **1978**, *8*, 317.

(14) Buys, H. R.; Geise, H. J. *Tetrahedron Lett.* **1968**, 5619.

(15) Bucourt, R. The Torsion Angle Concept in Conformational Analysis. *Topics in Stereochemistry*; Eliel, E. L., Allinger, N. L., Eds.; Interscience: New York, 1974; Vol. 8, p 159.

replaced[11] by a spherical polar set (P_2, Θ, Q), where Q is the total puckering amplitude

$$Q = \sqrt{\Phi_2^2 + \Phi_3^2} \tag{3}$$

and

$$\Theta = \arctan(\Phi_2/\Phi_3) \tag{4}$$

with $0 \leq \Theta \leq \pi$. This transformation allows one to map out the conformation of the ring on the surface of a sphere with radius Q and with poles at $\Theta = 0°$ and 180°; cf. Figure 2. The latter description of conformational space accessible to six-membered rings, originally proposed by Hendrickson,[16] is convenient and pictorial and will be used throughout this paper. For further ease, however, the TF parameters of the six-membered ring conformations at hand can also be translated into a rough classification in terms of the canonical conformations boat (B), twist-boat (T), chair (C), half-chair (H), and envelope (E). The approximate conformations are indicated by the appropriate capital letter and are further specified by superscript and/or subscript numerals distinguishing between the variants of each (e.g., ${}^1C_4$, ${}^4C_1$, etc.). The numerals are the locants of ring atoms that lie outside the reference plane defined by the remaining four coplanar ring atoms. The locants of ring atoms that lie "above" the reference plane (see also legend to Figure 1) are written as superscripts and precede the letter; those of the ring atoms that lie "below" the reference plane are written as subscripts and follow the letter. This notation concurs with the symbolic formalism introduced by Boeyens[13] which in turn is very similar to the IUPAC conformational nomenclature for six-membered ring forms of monosaccharides.[17,18]

In case all six endocyclic torsions (ϕ_j) are known, the TF-puckering coordinates Φ_2, P_2, and Φ_3 can be evaluated[11] by a simple Fourier inversion. If less (but more than 2) endocyclic torsion angles are available, the set of equations denoted by eq 2 may still be solved, e.g., by least-squares minimization techniques. The ϕ_j values needed for determining the puckering coordinates may be derived from NMR as follows. With the help of the generalized Karplus equation,[12] vicinal coupling constants can be translated into proton–proton torsion angles (ϕ_{HH}). The proton–proton torsion about an endocyclic bond is related to the corresponding endocyclic torsion by

$$\phi_{HH} = a + b\phi_j \tag{5}$$

Using the trigonal projection symmetry approximation, b will be 1 and a will be 0° for cis protons and ±120° for trans protons. Note that, since the H–C–H valence angle is known to be 1°–2° smaller than the tetrahedral value,[19] a projected H–C–H angle of 118° should be used. This entails a to be 0° (cis) or ±118° (trans) in CH_2–CH_2 fragments and ±1° (cis) or ±119° (trans) in CH_2–CH fragments.

By combining eq 2, eq 5, and the generalized Karplus equation,[12] the vicinal coupling constants about endocyclic bonds can be expressed as a function of the conformational parameters involved:

$$J_{HH} = f(\Phi_2, P_2, \Phi_3) \tag{6}$$

The latter function was implemented in a least-squares procedure (written in Turbo Pascal version 6.0, using an IBM PS/2, Model 70 computer) that calculates the best fit of Φ_2, P_2, and Φ_3 to the experimental ${}^3J_{HH}$ values (procedure I). As an optional feature the possibility to include known ϕ_j values in the experimental dataset was added to this procedure. This option is useful when one or more endocyclic torsions can be deduced directly from the chemical structure, e.g., an endocyclic double (or aromatic) bond ($\phi_j = 0°$). If the latter option is used, a weighting scheme[20] for the experimental input is employed in the minimization procedure in which observed coupling constants are assigned a relative weight of 1 and "observed" torsions are assigned a relative weight of 100.

Upon executing the procedure described above, some peculiarities were encountered. It turned out that, dependent on the starting values used for Φ_2, P_2, and Φ_3, the minimization may be rather easily trapped in some local minimum. In order to find the global minimum, one has to perform the calculation several times using start parameters that are systematically varied (in practice the eight combinations afforded by $\Phi_2 = 30°$, $P_2 = 0°/90°/180°/270°$, and $\Phi_3 = -30°/30°$ yield satisfactory results). Another case in point is that the "best" minimum found occasionally denotes a physically unrealistic ring conformation. Therefore, a few criteria (i.e., $\Phi_2 > 90°$, $|\Phi_3| > 80°$, any single $|\phi_j| > 80°$) are employed to reject such "best" solutions. These prescripts are built in into our standard operating procedure.

The "quality" of the best fit thus found by procedure I may be judged from the residual rms (root-mean-square) deviation between observed and calculated coupling constants. Typical rms values range from 0.2 to 0.6 Hz for a well-behaving single state situation. This corresponds reasonably well with what one expects on basis of the accuracy of the generalized Karplus equation[12] used. It is not easy to define rigorously a limit of acceptability; however, an rms ≥ 0.9 Hz is indicative of serious errors in the model (or the experimental couplings) used.

In case the validity of the model is doubted, a second model may be adopted in which the six-membered ring is assumed to be engaged in a fast two-state conformational equilibrium

$$(\Phi_2, P_2, \Phi_3) \rightleftarrows (\Phi_2', P_2', \Phi_3')$$

and where each conformational state is characterized by its own set of puckering coordinates. According to eq 1, the observed couplings now represent time-averaged coupling constants which are related to the couplings of the individual conformers and their relative populations in equilibrium:

$$J_{obs} = \alpha J + (1 - \alpha)J' \tag{7}$$

where α represents the mole fraction of the first conformer; J and J' represent the coupling constants belonging to the pure conformers, respectively. Combination of the generalized Karplus equation[12] and eqs 2, 5, and 7 gives ${}^3J_{HH}$ as a function of the conformational parameters involved:

$$J_{HH} = f(\Phi_2, P_2, \Phi_3, \alpha, \Phi_2', P_2', \Phi_3') \tag{8}$$

The problem boils down to determining the seven independent parameters Φ_2, P_2, Φ_3, α, Φ_2', P_2', and Φ_3' from the observed coupling constants. This objective was realized by an iterative least-squares minimization (written in Turbo Pascal, version 6.0) devised to obtain the best fit of equilibrium parameters to the experimental couplings. This procedure will be referred to as procedure II; note that the procedure also allows known ϕ_j values to be included in the experimental dataset.

A few comments on procedure II are in order. First, the same caveats as stated above for procedure I are valid for this procedure and are analogously taken care of. Second, the number of parameters (7) to be extracted from the experimental dataset will in general exceed the number of observed coupling constants and "observed" ϕ_j values. In that case the system is underdetermined and hence the number of parameters to be deduced from the experimental dataset must be reduced by constraining one or more parameters to fixed values.

Alternatively, if for a given system the equilibrium constant of the conformational two-state equilibrium can be influenced by changes in, e.g., temperature, pH, or solvent, then coupling constants may be determined under n different conditions. Assuming that the ring geometries in the conformational equilibrium are invariant under these changes in conditions, eq 8 can be extended to a set of n equations

$$J_{HH} = f(\Phi_2, P_2, \Phi_3, \alpha_i, \Phi_2', P_2', \Phi_3') \tag{9}$$

---

[16] Hendrickson, J. B. *J. Am. Chem. Soc.* **1967**, *89*, 7047.

[17] Rules for Conformation Nomenclature for Five- and Six-membered Rings in Monosaccharides and Their Derivatives. *J. Chem. Soc. Chem. Commun.* **1973**, 505.

[18] IUPAC-IUB Joint Commission on Biochemical Nomenclature. *Eur. J. Biochem.* **1980**, *111*, 295.

[19] Davis, M.; Hassel, O. *Acta Chem. Scand.* **1963**, *17*, 1181.

[20] Clifford, A. A. *Multivariate Error Analysis*; Applied Science Publishers Ltd.: London, 1973.

where $i = 1, ..., n$. Since each change in condition adds only one extra parameter (α_i) to be determined but usually several observables (J_{HH}) to the input dataset, the ratio observables versus parameters will thus be improved. The set of eq 9 can be solved by iterative least-squares minimization techniques; the latter type of minimization will be referred to as procedure III. Again, the procedure allows for known ϕ_j values to be included in the experimental dataset.

Of course, eq 9 can also be solved for a series of closely related molecules measured under similar conditions as long as the assumption holds that all molecules adopt very similar geometries in the conformational equilibria under study and only the molar ratio varies. However, for a successful application of procedure III it is essential that the variation in equilibrium constants span a substantial range. If this is not the case (for instance, if mole fractions vary, say, a mere 10%), then effectively only one set of couplings is used in the minimization, and procedure III will be bound to fail. The deficiency in experimental data can in that case only be compensated by reducing the number of parameters to be extracted from the input dataset. Preferably, this is done by constraining the puckering coordinates (Φ_2,P_2,Φ_3) of the less abundant and therefore less well-defined conformer to fixed values obtained from, e.g., solid-state data or molecular modelling.

As a final, more general remark it is noted that strictly speaking the above-described procedures interpret experimental coupling constants in terms of hypothetical motionless six-membered ring conformations occupying single points on the sphere describing conformational space; cf. Figure 2. But in reality, molecules possess, of course, a certain flexibility in the sense that within each potential energy pocket torsional motions will occur about the minimum resulting in an oscillation of the TF phase angle and puckering amplitudes. Therefore, the observed experimental couplings are, in fact, time averages over internal torsional/vibrational degrees of freedom, and the recently published CUPID method[21,22] advocates special measures to account for this phenomenon. However, studies involving five-membered ring conformations (where in general this effect is larger than in six-membered rings) have shown[23,24] that such "pseudolibration" motility, even when spanning a large range of the pseudorotational pathway, does not give rise to substantial changes in the coupling constants calculated. In analogy to the latter studies it is therefore expected that analyses performed along the lines of the procedures described in this paper may be taken to yield time-averaged solution structures for which the calculated TF parameters denote the center of the (probably anharmonic) continuous potential energy pocket of the conformation(s) at hand.

Results and Discussion

Scheme I

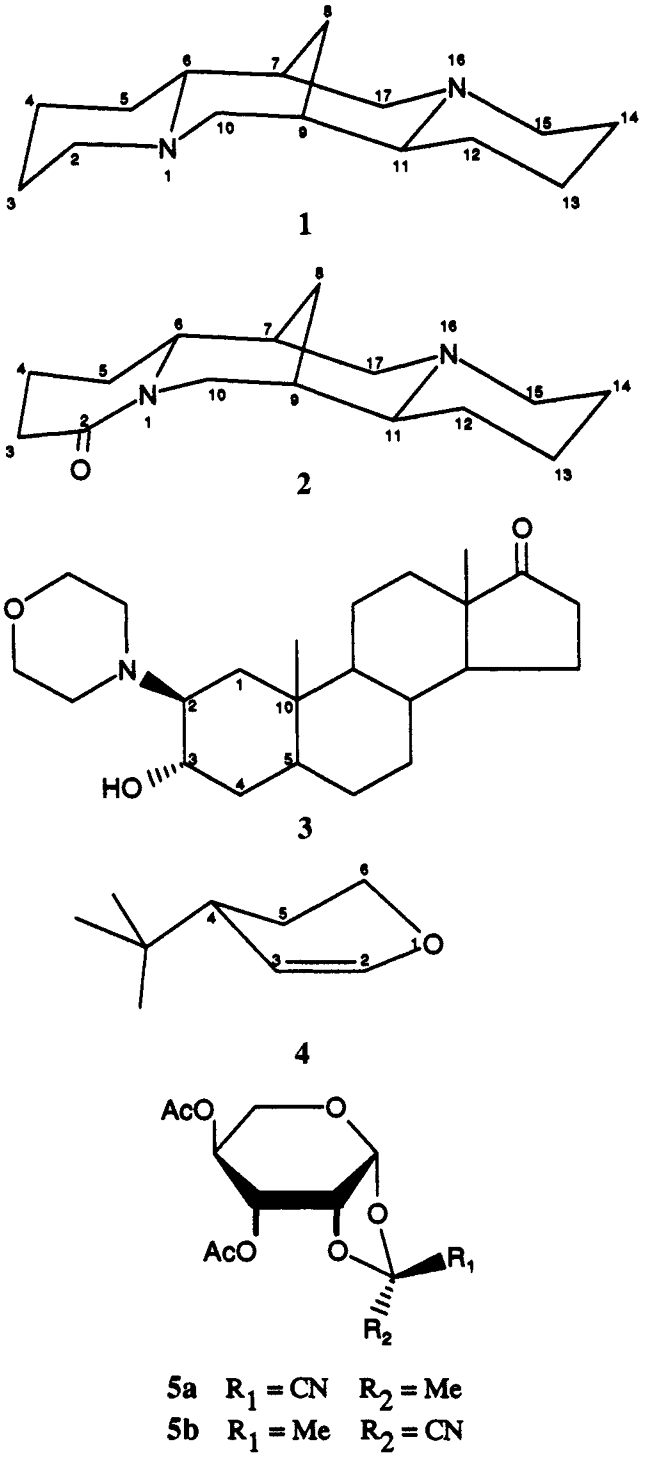

Sparteine. As a first test of the methodology described in this paper, the six-membered C ring of the sparteine skeleton was studied. Sparteine (**1**), lupanine (2-oxosparteine, **2**), and their analogues are tetracyclic alkaloids for which some 40 crystal structures are recorded in the Cambridge Structural Datafile.[25,26] Scrutiny of these structures shows that in about half of these reports ring C (formed by the atoms C_7–C_{17}–N_{16}–C_{11}–C_9–C_8) adopts a ^8C_N-chair conformation. However, except for two cases, there always appears to be a chemical incentive for such a chair conformation, e.g., substitution of N_{16} at the α-position or the two nitrogen atoms of sparteine ligating a single cation positioned at the α-side of the molecule. In the remaining 20 structures ring C adopts a $^{N,8}B$ boat-type conformation. The latter boat conformations are virtually identical as is evidenced by the very small standard deviations (2°–5°) in the TF parameters calculated for these rings. In order to determine whether the carbonyl group at position 2 in lupanine affects the boat conformation of the C ring in some systematic way, mean TF parameters were calculated for the C ring in sparteine (9 crystal structures) and lupanine (11 crystal structures) compounds; cf. Table I. As can be gleaned from Table I, the conformation of the C ring is very alike in both types of molecules. This is also borne out by molecular mechanics (MM) calculations performed for both sparteine and lupanine: the TF parameters of the C ring in these calculated structures

---

(21) Dzakula, Z.; Westler, W. M.; Edison, A. S.; Markley, J. L. *J. Am. Chem. Soc.* **1992**, *114*, 6195.

(22) Dzakula, Z.; Westler, W. M.; Edison, A. S.; Markley, J. L. *J. Am. Chem. Soc.* **1992**, *114*, 6200.

(23) Haasnoot, C. A. G.; Leeuw, F. A. A. M. de; Leeuw, H. P. M. de; Altona, C. *Org. Magn. Reson.* **1981**, *15*, 43.

(24) Leeuw, F. A. A. M. de; Altona, C.; Kessler, H.; Bermel, W.; Friedrich, A.; Krach, G.; Hull, W. E. *J. Am. Chem. Soc.* **1983**, *105*, 2237.

(25) Allen, F. H.; Kennard, O.; Taylor, R. *Acc. Chem. Res.* **1983**, *16*, 146.

(26) Allen, F. H.; Bellard, S.; Brice, M. D.; Cartwright, B. A.; Doubleday, A.; Higgs, H.; Hummelink, T.; Hummelink-Peters, B. G.; Kennard, O.; Motherwell, W. D. S.; Rodgers, J. R.; Watson, D. G. *Acta Cryst.* **1979**, *B35*, 2331.

(27) Allinger, N. L. *J. Am. Chem. Soc.* **1977**, *99*, 8127.

(28) MM2 Programme, Version 1987; ex Molecular Design Ltd., 2132 Farallon Dr., San Leandro, CA 94577.

Table I. TF Puckering Coordinates (deg) and Coupling Constant Data (Hz) for Ring C in Sparteine (**1**) and Lupanine (**2**)

TF parameters	sparteine			lupanine		
	X-ray[a]	MM2[b]	proc I[c]	X-ray[d]	MM2[b]	proc I[c]
Φ_2	64.8	66.6	59.7	64.8	66.3	58.7
P_2	150.0	149.3	148.3	154.2	146.6	146.3
Φ_3	−4.2	−3.3	−6.3	−3.0	−1.4	−7.4
Θ	93.7	92.8	96.0	92.7	91.2	97.3
Q	65.1	66.6	60.1	64.9	66.3	59.2
couplings	J_{obs}[e]	J_{calc}[c]	ΔJ[c]	J_{obs}[e]	J_{calc}[c]	ΔJ[c]
H_7–$H_{17\alpha}$	3.9	3.7	0.2	3.8	3.9	−0.1
H_7–$H_{17\beta}$	10.8	9.7	1.1	10.0	9.8	0.2
H_9–H_{11}	2.1	2.6	−0.5	2.2	2.2	0.0
$H_{8\alpha}$–H_9	3.8	3.3	0.5	3.2	3.1	0.1
$H_{8\beta}$–H_9	2.5	3.0	−0.5	3.2	3.1	0.1
H_7–$H_{8\alpha}$	2.4	3.5	−1.1	3.8	3.7	0.1
H_7–$H_{8\beta}$	2.5	2.7	−0.2	2.8	2.6	0.2
rms dev			0.69			0.14

[a] Mean values determined from nine crystal structures of sparteine compounds (see text). [b] Determined from the energy minimized structure using the MM2 molecular mechanics program.[27,28] [c] Results obtained from coupling constant analysis (procedure I); see text. [d] Mean values determined from 11 crystal structures of lupanine compounds (see text). [e] Taken from ref 29.

are very similar to each other and, in turn, also very similar to the mean values of the TF puckering coordinates obtained from the crystal structures (see Table I). Hence, it may be concluded that the conformation of the C ring is not influenced by substitution of the C_2 position of the sparteine skeleton.

In 1986, Golebiewski[29] reported the vicinal NMR coupling constants of sparteine and lupanine as determined by 2D *J*-resolved NMR techniques. These couplings were analyzed by means of procedure I (vide supra), and the results of the analyses for the C ring are summarized in Table I. For sparteine a best fit between experimental and calculated couplings was obtained for a C ring conformation characterized by P_2 = 148.3°, Θ = 96.0°, and Q = 60.1°, i.e., a $^{N,8}B$ conformation. The latter TF parameters point to a slightly less puckered C ring in solution but are for the rest in excellent agreement with the ring puckering coordinates obtained from X-ray data and MM calculations (cf. Table I). However, the overall correspondence between observed and calculated coupling constants seems much less satisfactory (rms deviation 0.69 Hz). As was dwelt upon in the previous section, such a large rms deviation might be indicative of an error in the model used. Therefore, the coupling constant data were reanalyzed in terms of a two-state conformational equilibrium (procedure II). It was found that the introduction of a second conformer cannot improve the correspondence between observed and calculated couplings. Hence, it must be concluded that, notwithstanding the rather large discrepancy between calculated and observed coupling constants, ring C of sparteine adopts exclusively a $^{N,8}B$ conformation in solution.

Although the coupling constants reported[29] for lupanine (**2**) differ substantially from those reported for sparteine, an analysis of the lupanine couplings along the lines of procedure I arrives at a $^{N,8}B$ conformation (P_2 = 146.3°, Θ = 97.3°, Q = 59.2°) for its C ring that is virtually indistinguishable from the one found for the sparteine C ring (cf. Table I). This finding corroborates the conclusion drawn from X-ray data and MM calculations (vide supra) that substitution at C_2 does not influence the C ring conformation. Moreover, worth commenting is the rms deviation between observed and calculated couplings which is much better in the lupanine (0.14 Hz) than in the sparteine case (0.69 Hz). From the experimental details given by Golebiewski,[29] it can be deduced that the digital resolution in the f_1-slices of the 2D *J*-resolved spectra is about 0.5 Hz. Furthermore, the author mentions that most coupling constants were extracted from the spectra using a first-order approximation. Taken together, the conclusion seems justified that the accuracy of the experimental couplings is considerably worse than the 0.3 Hz claimed.[29] Seen in this light, the very high rms deviation between observed and calculated couplings for sparteine (and probably also the surprisingly low corresponding rms deviation for lupanine) may well be ascribed to random errors in the experimental ^3J dataset. This being the case, it might be inferred that the methodology presented in this paper is not very sensitive to random errors in the experimental coupling constants.

3α-Hydroxy-2β-(4-morpholinyl)-5α*H*-androstan-17-one (3). Recently, Fielding and Grant[30] reported an NMR and molecular mechanics study of **3**. From comparison of the coupling constants calculated on basis of MM structures with the experimental ones, it was concluded that the conformation of ring A (formed by C_1–C_{10}–C_5–C_4–C_3–C_2) depends of the polarity of the solvent, i.e., a $^{10}C_3$ chair in DMSO versus a $^{10}T_2$ twist-boat in $CDCl_3$ solution.

When the ring A coupling constants observed in DMSO solution are reanalyzed by means of procedure I, an excellent fit between observed and calculated couplings (rms deviation 0.17 Hz) is found for P_2 = 253.5°, Θ = 179.7°, Q = 56.2°, i.e., for all practical purposes a perfect $^{10}C_3$ chair conformation. Judging purely by the numbers, the latter P_2 value differs substantially from the one predicted by MM2[28] (cf. Table II). However, one should bear in mind that in the least-squares procedure I the standard deviation (σ) of P_2 becomes very large at very low magnitudes of Φ_2; for the perfect chair (Φ_2 = 0°), the case is carried into extremes as the value of P_2 becomes irrelevant. In the case at hand, the standard deviation of P_2 is calculated to be 179°; hence the P_2 value predicted by MM2 is within its range. Seen in this light, the correspondence between the conformation deduced from the NMR coupling constants and the one predicted by MM2 is quite good. The differences in overall conformation are minor and fall within the combined error limits inherent to both methods.

The coupling constants determined for ring A in $CDCl_3$ solution are examined next. Presuming a single conformation (procedure I), a $^{10}T_2$ twist-boat conformation, characterized by P_2 = 61.4°, Θ = 94.0°, Q = 61.6°, is indicated for ring A. Such a conformation agrees very well with the twist-boat conformation predicted for this ring by MM2[28] (cf. Table II). However, the residual rms difference between experimental and calculated couplings (0.70 Hz) is quite high. Therefore, the coupling constants were reanalyzed assuming a two-state conformational equilibrium (procedure II). In order to reduce the degrees of freedom in the fitting procedure, the assumption was made that one of the constituent conformations would be the one occurring in DMSO solution (vide supra). Applying this constraint to the fitting procedure leads to a roughly 9:1 equilibrium between $^{10}T_2$ and $^{10}C_3$ conformations for ring A (cf. Table II). Remarkably, the introduction of a second (chair) conformer has virtually no effect on the TF parameters calculated for the twist-boat conformation. This shows that the two conformers are not correlated; in other words, the extra degree of freedom introduced by the $^{10}C_3$ conformation is orthogonal to the one by the $^{10}T_2$ conformer. On the other hand, the reduction in rms deviation between observed and calculated couplings when going from procedure I to procedure II is rather small (0.70 Hz versus 0.57 Hz) and throws some doubts on the pertinence of the $^{10}C_3$ conformer. Hence, an unambiguous choice between the two possibilities delineated by procedure I and II, respectively, cannot be made at present. It is reasonable to state that the major A ring conformer in $CDCl_3$ solution corresponds to a $^{10}T_2$ twist-boat conformation. The presence of a small amount (0–9%) of a $^{10}C_3$ form cannot be precluded; the calculations presented above mark the boundaries for the conformational ranges.

4-*tert*-Butyl-5,6-dihydro-4*H*-pyran (4). The double bond in the six-membered dihydropyran ring is supposed[32] to force **4** into a $^6H_5$ half-chair conformation. MM2 calculations endorse this assumption as we find a minimum energy conformation characterized by P_2 = 114.9°, Θ = 132.7°, Q = 43.5°.

Although the vicinal coupling constants about three endocyclic bonds are available,[32] it should be realized that the generalized

---

(29) Golebiewski, W. M. *Magn. Reson. Chem.* **1986**, *24*, 105.

(30) Fielding, L.; Grant, G. H. *J. Am. Chem. Soc.* **1991**, *113*, 9785.

(31) Allinger, N. L.; Yuh, Y. H. *QCPE* **1980**, *12*, 395.

Table II. Puckering Coordinates (deg) and Coupling Constant Data (Hz) for Ring A in 3α-Hydroxy-2β-(4-morpholinyl)-5α*H*-androstan-17-one (**3**)

	3 in DMSO			3 in CDCl$_3$				
TF parameters	MM ($^{10}C_3$)[a]	procedure I[b]		MM ($^{10}T_2$)[a]	procedure I[b]		procedure II[c]	
Φ_2	1.8	0.3		59.9	61.4		61.5	0.3
P_2	114.9	253.5		-54.1	-53.9		-53.8	253.5
Φ_3	-56.0	-56.2		-0.1	-4.3		-3.2	-56.2
Θ	178.2	179.7		90.1	94.0		93.0	179.7
Q	56.1	56.2		59.9	61.6		61.6	56.2
mol fraction		(1.0)			(1.0)		0.91	0.09
couplings	J_{obs}[a]	J_{calc}[b]	ΔJ[b]	J_{obs}[a]	J_{calc}[b]	ΔJ[b]	J_{calc}[c]	ΔJ[c]
$H_{1\alpha}$–$H_{2\alpha}$	3.1	3.2	-0.1	7.4	7.7	-0.3	7.2	0.2
$H_{1\beta}$–$H_{2\alpha}$	2.9	3.0	-0.1	8.9	9.2	-0.3	8.8	0.1
$H_{2\alpha}$–$H_{3\beta}$	3.0	3.0	0.0	9.5	9.5	0.0	8.9	0.6
$H_{3\beta}$–$H_{4\alpha}$	3.4	3.4	0.0	5.8	6.4	-0.6	6.3	-0.5
$H_{3\beta}$–$H_{4\beta}$	2.5	2.5	0.0	7.8	9.2	-1.4	8.5	-0.7
$H_{4\alpha}$–$H_{5\alpha}$	3.7	3.6	0.1	6.8	6.2	0.6	6.1	0.7
$H_{4\beta}$–$H_{5\alpha}$	12.7	12.3	0.4	11.9	11.1	0.8	11.1	0.8
rms dev			0.17			0.70		0.57

[a] Observed coupling constants and structures were taken from Fielding and Grant.[30] Present structures were recalculated by MM2 (1987 version).[28] It is noted that in the latter force field the difference in steric energy between the two conformers amounts to 0.07 kcal/mol, i.e., considerably less than the 2.3 kcal/mol originally reported using the 1977 version of MM2.[31] [b] Results obtained from analyzing experimental coupling constants of ring A by means of procedure I. [c] Puckering coordinates and theoretical couplings for ring A engaged in a two-state conformational equilibrium as calculated by procedure II. In this minimization the TF parameters (Φ_2, P_2, Φ_3) of the minor $^{10}C_3$ conformer were constrained to the conformation determined by procedure I for the DMSO solute (see text).

Table III. Puckering Coordinates (deg) and Coupling Constant Data (Hz) for 4-*tert*-Butyl-5,6-dihydro-4*H*-pyran (**4**)

TF parameters	MM ($^6H_5$)[a]	MM ($^5H_6$)[a]	procedure I[b]		procedure II[c]		procedure II[d]	
Φ_2	32.0	29.6	32.7		32.0	43.3	30.6	29.6
P_2	114.9	-60.7	132.6		114.9	-17.2	122.8	-60.7
Φ_3	-29.5	26.7	-31.9		-29.5	31.8	-30.6	26.7
Θ	132.7	48.0	134.3		132.7	53.7	134.0	48.0
Q	43.5	39.8	45.7		43.5	53.8	43.3	39.8
mol fraction			(1.0)		0.89	0.11	0.91	0.09
couplings		J_{obs}[e]	J_{calc}[b]	ΔJ[b]	J_{calc}[c]	ΔJ[c]	J_{calc}[d]	ΔJ[d]
H_4–H_5		5.5	6.0	-0.5	5.4	0.1	5.6	-0.1
H_4–$H_{5'}$		10.5	11.3	-0.8	10.7	-0.2	10.6	-0.1
H_5–H_6		1.9	1.5	0.4	1.9	0.0	2.0	-0.1
H_5–$H_{6'}$		3.3	2.7	0.6	3.3	0.0	3.2	0.1
$H_{5'}$–H_6		11.2	11.8	-0.6	11.0	0.2	11.0	0.2
$H_{5'}$–$H_{6'}$		3.5	3.0	0.5	3.2	0.3	3.3	0.2
rms dev				0.59		0.20		0.14

[a] Puckering coordinates of the structures calculated by means of MM2 (1987 version).[28] [b] Results obtained from coupling constant analysis using procedure I. [c] Puckering coordinates and theoretical couplings for **4** engaged in a two-state conformational equilibrium as calculated by procedure II. In this minimization the TF parameters (Φ_2, P_2, Φ_3) of the major $^6H_5$ conformer were constrained to the $^6H_5$ conformation predicted by MM2. [d] As in footnote *c*, but now the TF parameters (Φ_2, P_2, Φ_3) of the minor $^5H_6$ conformer were constrained to the $^5H_6$ conformation predicted by MM2. [e] Taken from ref 32.

Karplus equation[12] has only been parametrized for $C(sp^3)$–$C(sp^3)$-type bonds, and hence the reported $^3J(H_3$–$H_4)$ about the $C_3(sp^2)$–$C_4(sp^3)$ bond cannot be used for purposes of conformational analysis. However, the endocyclic torsion about the C_2–C_3 double bond can safely be assigned to 0° which then provides the third torsion angle needed in the present analyses (cf. Procedures). Analysis of the coupling constants in terms of a single-state conformation by means of procedure I leads to a conformer described by $P_2 = 132.6°$, $\Theta = 134.3°$, $Q = 45.7°$, i.e., an intermediate conformation between $^6H_5$ and ^6E (cf. Table III). At first sight this seems to be an acceptable solution; the difference between the latter conformation and the one predicted by MM2 is a matter of degree, not of kind. Moreover, the residual rms deviation between observed and calculated couplings (0.59 Hz), although fairly high, is still acceptable. Scrutiny of the individual couplings (see Table III), however, reveals that the two calculated trans (pseudo-) diaxial couplings, $^3J(H_4$–$H_{5'})$, and $^3J(H_{5'}$–$H_6)$, exceed the observed ones by 0.6–0.8 Hz. Since this might indicate that the observed coupling constants in reality represent a conformational equilibrium in which the trans diaxial couplings are time-averaged with corresponding trans diequatorial couplings, the possibility of such a conformational equilibrium was examined next. In order to reduce the number of parameters to be extracted from the experimental couplings, it was assumed that one of the constituent conformers corresponds to the one predicted by MM2. Under this constraint procedure II smoothly converges to a 9:1 equilibrium between a $^6H_5$ and an $E_6/^1H_6$ ($P_2 = -17.2°$, $\Theta = 53.7°$, $Q = 53.8°$) conformation, and as can be gleaned from Table III the correspondence between observed and calculated coupling constants improved considerably for this minimization.

MM2 calculations were performed to underpin the plausibility of a two-state conformational equilibrium, and, indeed, a second (local) energy minimum conformation ($^5H_6$, $P_2 = -60.7°$, $\Theta = 48.0°$, $Q = 39.8°$) was found. The difference in MM2 steric energy between the calculated $^6H_5$ and $^5H_6$ conformations amounts to 2.2 kcal in favor of the former, thereby indicating that an equilibrium between the two will be strongly biased toward the $^6H_5$ conformer. The latter finding corroborates the $^3J_{HH}$ = analysis according to procedure II (vide supra), but the correspondence in puckering coordinates derived by the two methods is less satisfactory (cf. Table III).

At this point it should be realized that in the $^3J_{HH}$ analysis presented above the conformation of the most abundant conformer was kept rigid. This implies that the minimization procedure can only influence the calculated, averaged $^3J_{HH}$ values by varying the minor component's conformation and population. Since the

---

(32) DeBoer, A. *Org. Magn. Reson.* **1973**, *5*, 7.

Table IV. Puckering Coordinates (deg) and Coupling Constant Data (Hz) for **5a**

TF parameters		X-ray[a]		procedure I[b]		procedure II[c]	
Φ_2		60.0		67.7		67.9	10.3
P_2		122.9		133.6		133.7	263.4
Φ_3		−4.1		−7.4		−7.7	53.4
Θ		93.9		96.2		96.4	10.9
Q		60.2		68.1		68.4	54.4
mol fraction		(1.0)		(1.0)		0.98	0.02
couplings	J_{obs}[d]	J_{calc}[a]	ΔJ[a]	J_{calc}[b]	ΔJ[b]	J_{calc}[c]	ΔJ[c]
H_1–H_2	5.4	4.7	0.7	5.6	−0.2	5.6	−0.2
H_2–H_3	2.8	2.9	−0.1	2.6	0.2	2.6	0.2
H_3–H_4	7.7	5.8	1.9	7.5	0.2	7.5	0.2
H_4–H_{5a}	5.3	4.6	0.7	5.4	−0.1	5.4	−0.1
H_4–H_{5e}	1.5	1.3	0.2	1.4	0.1	1.6	−0.1
rms dev			0.95		0.19		0.16

[a] TF parameters and coupling constants calculated for the X-ray structure[33,34] of **5a** (see text). [b] Puckering coordinates and calculated couplings obtained from coupling constant analysis using procedure I. [c] Puckering coordinates and coupling constants calculated for **5a** assuming a two-state conformational equilibrium (procedure II) in which the TF parameters for the minor conformer (last column) are constrained to the values calculated for the chair conformation observed for **5b** in the solid state. [d] Taken from ref 33.

minor conformation occurs for only about 10%, there is a high leverage effect due to which the errors propagated to the derived puckering coordinates of the minor conformer are considerable. This is reflected in the high standard deviations (σ) calculated for the puckering coordinates derived for the second conformer: $\sigma(\Phi_2) = 21.5°$, $\sigma(P_2) = 26.4°$, and $\sigma(\Phi_3) = 6.6°$.

In the Procedures section the recommendation was made that in case puckering coordinates have to be constrained in the minimization procedure, the less abundant conformer's ones should be fixed. To illustrate this point, the $^3J_{HH}$ analysis using procedure II was repeated but now with the puckering coordinates of the minor conformer constrained to the values pertaining to the MM2 $^5H_6$ (local) minimum energy structure (cf. Table III). Now, a biased two-state equilibrium between $^6H_5$ (91%) and $^5H_6$ (9%) ring conformations is found. The puckering coordinates derived for the $^6H_5$ conformer agree very well with the ones predicted for this conformer by MM2 (cf. Table III). Moreover, the standard deviations calculated for these puckering coordinates are considerably smaller than in the previous $^3J_{HH}$ analysis, being $\sigma(\Phi_2) = 1.2°$, $\sigma(P_2) = 4.9°$, and $\sigma(\Phi_3) = 1.1°$.

Taken together, in contrast to the original evaluation,[32] the $^3J_{HH}$ analyses as well as the molecular mechanics calculations presented above show that the six-membered ring of **4** is engaged in a (biased) two-state conformational equilibrium. It may therefore be concluded that a *tert*-butyl group is not able to block the dihydropyran ring in one single conformation.

3,4-Di-*O*-acetyl-1,2-*O*-(1-cyanoethylidene)-*β*-L-lyxopyranose (5a and 5b). Cano et al.[33] studied the conformation of **5a** and **5b** by X-ray diffraction and NMR techniques. They reported that in the solid state **5a** takes up a $^OT_2$ conformation[34] ($P_2 = 122.9°$, $\Theta = 93.9°$, $Q = 60.2°$), whereas the *R* isomer (**5b**) was shown to adopt a $^1C_4$ conformation ($P_2 = 263.4°$, $\Theta = 10.9°$, $Q = 54.4°$). The authors[33] used these solid-state conformations to interpret their NMR data and concluded that the observed couplings of **5a** could be accounted for by a major (90% of the conformer population) $^OT_2$ conformation with a small contribution of the $^1C_4$ conformer or small distortions in the ring.

Using the TF parameters calculated for the reported solid-state ring geometry of **5a**, the coupling constants expected for this conformation were computed using eq 2, eq 5, and the generalized Karplus equation[12] (cf. Table IV). These data show that the correspondence between calculated and observed coupling constants is poor (rms deviation 0.95 Hz). However, a $^3J_{HH}$ analysis by means of procedure I reveals that a good agreement (rms deviation 0.19 Hz) is obtained for an intermediate $^OT_2/^{O,3}B$ conformation ($P_2 = 133.6°$, $\Theta = 96.2°$, $Q = 68.1°$) of the pyranoid ring; see Table IV. The latter conformation is very akin to the one determined for **5a** by X-ray diffraction; compared to the latter it is only slightly more puckered and somewhat pseudorotated toward a $^{O,3}B$ conformation. Such relatively small differences may well be ascribed to crystal packing forces effective in the solid state.

In a final model calculation for **5a** the possibility of a chair-(twist-)boat conformational equilibrium was examined. Table IV reproduces the results for a $^3J_{HH}$ analysis using procedure II in which the chair conformer was fixed to the $^1C_4$ chair conformation observed for **5b** in the crystal. The best fit between experimental and calculated couplings was obtained for an almost completely one-sided equilibrium: the same $^OT_2/^{O,3}B$ conformation determined in the previous analysis is found, and this conformer accounts for 98% of the conformer population. Since the rms deviation between observed and calculated couplings (0.16 Hz) improved only marginally in comparison to the previous (single state) analysis, the significance of the contribution by the $^1C_4$ conformer to the conformational equilibrium may well be doubted. It is therefore concluded that in solution **5a** adopts virtually exclusively an intermediate conformation between $^OT_2$ and $^{O,3}B$.

When the coupling constants observed for **5b** at 25 °C were subjected to an analysis implying a single conformational state for the pyranoid ring (procedure I, results not shown), the rms deviation between observed and calculated couplings remained unacceptably high ("best" fit: 1.75 Hz rms deviation). This finding dismisses the suitability of such a single-state model, and therefore the conformational analysis of **5b** was escalated to a two-state equilibrium model.

In contrast to **5a**, the experimental coupling constants of **5b** turned out to be temperature dependent. The reported[33] changes in $^3J_{HH}$ upon going from 298 K to 173 K are considerable (up to 3.6 Hz) and seem indicative for appreciable changes in some conformational equilibrium. Therefore, the five coupling constant datasets measured for **5b** in the above-mentioned temperature range were analyzed according to procedure III, i.e., a two-state conformational equilibrium for which it is assumed that only the equilibrium constant changes as a function of temperature. In the case at hand, this means that 11 parameters (6 puckering coordinates and 5 equilibrium constants) are to be determined from 25 observed coupling constants. This overdetermined least-squares problem readily converged (overall rms deviation between observed and calculated couplings: 0.32 Hz); the results of the refinement are summarized in Table V. A perusal of the data presented in this table reveals that **5b** is indeed involved in a conformational equilibrium between a $^1C_4$-like and a $^OT_2$-like conformation. The geometry of the latter conformers show a striking conformity with the crystal structure data obtained for **5b** and **5a**, respectively.

The conformational analysis of **5b** can now be taken even one step further as the variation in mole fractions of the constituent conformers as a function of temperature allows an estimate of

---

[33] Cano, F. H.; Foces-Foces, C.; Jimenez-Barbero, J.; Alemany, A.; Bernabe, M.; Martin-Lomas, M. *Carbohydr. Res.* **1988**, *175*, 119.

[34] Note that two independent molecules were found to be present in the unit cell of **5a**. However, one of these molecules is supposed to be an average between two conformations in the crystal and is therefore left out of consideration in this paper.

Table V. Puckering Coordinates (deg) and Coupling Constant Data (Hz) Calculated Using Procedure III for a Series of Temperature-Dependent NMR Experiments[33] for **5b** Assuming a Two-State Conformational Equilibrium

TF parameters	conformer 1 ($^1C_4$)	conformer 2 ($^OT_2$)	TF parameters	conformer 1 ($^1C_4$)	conformer 2 ($^OT_2$)
Φ_2	10.5	62.5	Θ	10.2	90.7
P_2	269.9	131.5	Q	59.6	62.5
Φ_3	58.7	−0.8			

	T, 25 °C; mol fraction $^1C_4$ = 0.39			*T*, −20 °C; mol fraction $^1C_4$ = 0.56			*T*, −40 °C; mol fraction $^1C_4$ = 0.63			*T*, −60 °C; mol fraction $^1C_4$ = 0.70			*T*, −100 °C; mol fraction $^1C_4$ = 0.80		
couplings	J_{obs}	J_{calc}	ΔJ	J_{obs}	J_{calc}	ΔJ	J_{obs}	J_{calc}	ΔJ	J_{obs}	J_{calc}	ΔJ	J_{obs}	J_{calc}	ΔJ
H_1-H_2	3.8	3.9	−0.1	3.3	3.4	−0.1	3.1	3.2	−0.1	2.8	3.0	−0.2	2.7	2.7	0.0
H_2-H_3	3.1	2.9	0.2	3.3	3.1	0.2	3.3	3.2	0.1	3.4	3.3	0.1	3.5	3.4	0.1
H_3-H_4	8.2	8.5	−0.3	9.0	8.8	0.2	9.3	8.9	0.4	9.4	9.1	0.3	9.7	9.3	0.4
H_4-H_{5e}	4.5	5.3	−0.8	5.2	4.9	0.3	5.2	4.7	0.5	5.1	4.5	0.6	3.8	4.2	−0.4
H_4-H_{5a}	4.9	5.2	−0.3	6.6	6.6	0.0	7.3	7.3	0.0	7.9	7.9	0.0	8.5	8.8	−0.3
rms dev			0.41			0.21			0.30			0.33			0.30

the thermodynamic parameters for the apparent $^1C_4$–$^OT_2$ equilibrium. Thus, the following results were obtained from an Arrhenius plot (ln *K* versus 1/*T*): $\Delta H°$ = 1.5 kcal/mol and $\Delta S°$ = 5.4 eu. The latter data show that the $^1C_4$ conformer predominates at low temperatures for enthalpic reasons, whereas at ambient temperature the entropic contribution to the free energy difference favors the $^OT_2$ conformation of the pyranoid ring.

To the best of our knowledge, the present study represents the first experimental determination of the entropy difference between a chair and a twist-boat conformation for a carbohydrate molecule. As such, it is indicated that "steric" energy differences between chair and (twist-)boat conformations of carbohydrate molecules calculated by molecular mechanics methods should be corrected for an entropic contribution to the free energy of 1.5–2 kcal/mol in favor of the (twist-)boat conformer when comparing them to experimental equilibrium data obtained at ambient temperature.

Acetylated Glycals 6–12 (cf. Table VI). The proton NMR data for a series of 1,2-unsaturated glycopyranoses (**6–12**) have been reported by Rico and Santoro.[35] These authors analyzed their coupling constant data using a least-squares computer procedure assuming that compounds **6–12** undergo a rapid interconversion between $^4H_5$ and $^5H_4$ conformers. Furthermore, most of the limiting $^3J_{HH}$ values about corresponding bonds in the latter constituent conformers were assumed to be equal. The first assumption seems reasonable, but, in view of the gross differences in (configurational) substituent patterns of compounds **6–12**, the last assumption is not warranted.[12] Therefore, a reanalysis of the vicinal coupling constant dataset is called for.

However, a conformational analysis along the lines of procedure II for each of the individual compounds **6–12** seems a perilous undertaking since only two (**8–12**) to maximally three (**6**, **7**) couplings are available in each compound from which information about two of the endocyclic torsions (ϕ_3 and ϕ_4) have to be extracted. Of course, the double bond between C_1 and C_2, present in all compounds, delivers the necessary information (ϕ_1 = 0°) about a third endocyclic torsion, but this does not resolve the rather feeble basis of the calculational problem.

As an alternative, the applicability of procedure III was investigated. To this end, MM2[28] calculations were performed for the $^4H_5$ and $^5H_4$ conformations of compounds **7**, **10**, and **11**. It was found that the aforementioned two conformers are virtually identical in all three compounds as is reflected by the very narrow range in the TF parameters calculated from the MM2 structures ($^4H_5$: P_2 = 54° ± 2°, Θ = 133° ± 1°, Q = 42° ± 2°; $^5H_4$: P_2 = 230° ± 3°, Θ = 47° ± 0°, Q = 42° ± 1°). Hence, it is indicated that compounds **6–12** are engaged in very similar two-state equilibria in which only the equilibrium constants may vary from compound to compound. This being the case, a $^3J_{HH}$ analysis by means of procedure III seems appropriate. Indeed, a good correspondence between observed and calculated couplings (Table VI, overall rms deviation 0.35 Hz) was obtained in this way for an equilibrium between $^4H_5$ (P_2 = 69.0°, Θ = 134.6°, Q = 45.1°) and $^5H_4$ (P_2 = 238.2°, Θ = 45.0°, Q = 37.6°) conformers. The one exception to this general statement is the H_4–H_5 coupling in **10** which is calculated to be 1.3 Hz smaller than actually determined. It is suggested that this discrepancy is to be attributed to an experimental artifact: the H_5 proton in **10** is virtually isochronous with the H_6 proton (chemical shift difference[35] = 0.004 ppm = 0.36 Hz!), and it is well conceivable that the complications arising from second-order effects have led to an erroneous value for this particular H_4–H_5 coupling.

Table VI. Experimental[35] and Calculated Coupling Constants (Hz) for a Series of Acetylated Glycals (**6–12**) Assuming a Two-State Conformational Equilibrium (Procedure III; See Text)

Compound		Coupling	J_{obs}	J_{calc}	ΔJ	$[^4H_5] \rightleftarrows [^5H_4]$
6	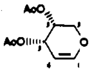	H_3-H_4	4.12	4.34	-0.22	0.84 : 0.16
		H_4-H_5	9.42	9.31	0.11	
		H_4-$H_{5'}$	3.57	3.92	-0.35	
		rms deviation			0.25	
7	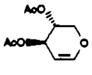	H_3-H_4	2.87	2.51	0.36	0.15 : 0.85
		H_4-H_5	3.24	3.49	-0.25	
		H_4-$H_{5'}$	1.96	2.00	-0.04	
		rms deviation			0.25	
8	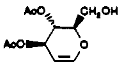	H_3-H_4	5.79	6.13	-0.34	0.72 : 0.28
		H_4-H_5	7.75	7.48	0.27	
		rms deviation			0.31	
9	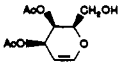	H_3-H_4	4.62	4.41	0.21	0.72 : 0.28
		H_4-H_5	1.76	1.78	-0.02	
		rms deviation			0.15	
10	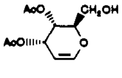	H_3-H_4	3.92	4.37	-0.45	1.00 : 0.00
		H_4-H_5	11.01	9.71	1.30	
		rms deviation			0.97	
11	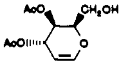	H_3-H_4	2.39	2.65	-0.26	0.86 : 0.14
		H_4-H_5	1.52	1.18	0.34	
		rms deviation			0.30	
12	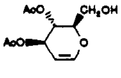	H_3-H_4	4.27	4.48	-0.21	0.46 :0.54
		H_4-H_5	5.55	5.38	0.17	
		rms deviation			0.19	
		Overall rms deviation			0.35	

Comparison of the puckering coordinates derived from the $^3J_{HH}$ analysis using procedure III and the ones predicted by MM2 (vide supra) show that both methods yield mutually consistent results. It is concluded that the present conformational analysis is in keeping with the view that the six-membered rings in **6–12** are involved in a conformational equilibrium between identical half-chair forms and that only the populations of the constituent conformers vary from compound to compound (cf. Table VI).

Conclusion

The application of the generalized Karplus equation[12] in combination with the Truncated Fourier formalism for six-membered rings[11] allows the elucidation of the relevant conformational pa-

---

[35] Rico, M.; Santoro, J. *Org. Magn. Reson.* **1976**, *8*, 49.

1468 *J. Am. Chem. Soc.* **1993**, *115*, 1468–1478

rameters of six-membered ring compounds from observed endocyclic vicinal proton–proton coupling constants. It is demonstrated that the computational procedures devised for this purpose lead to a consistent and quantitative conformational interpretation of a wide variety of six-membered ring compounds in solution. The latter interpretations are shown to correspond well to conformational data obtained for these compounds by other techniques such as X-ray crystallography and/or molecular mechanics. Moreover, the present analysis can detect whether the six-membered ring occurs in a fast two-state conformational equilibrium and, if so, describe that equilibrium quantitatively. It is therefore concluded that conformational analyses performed along the lines of the methods presented in this paper are capable of increasing our detailed and *quantitative* understanding of the conformational behavior of six-membered rings in solution to a level not heretofore attained.

Polarizability and Nuclear Shielding for the Sodium Anion in Condensed Phases

N. C. Pyper,[†] **C. G. Pike,**[†] **and P. P. Edwards***[,‡]

Contribution from the University Chemical Laboratory, Lensfield Road, Cambridge CB21 EW, U.K., and The School of Chemistry, University of Birmingham, Edgbaston, Birmingham B15 2TT, U.K. *Received August 26, 1992*

Abstract: The environmental modifications of the polarizability, the diamagnetic contribution to the susceptibility, and the nuclear shielding of the sodium anion (Na^-) in the cryptand salt $Na^-\cdot Na^+C_{222}$ (C_{222} = cryptand 222) are deduced from ab-initio quantum chemistry computations. The point charge electrostatic contribution to the anion environment in the cryptand reduces to 643 au, the free anion polarizability of 1090 au predicted taking account of electron correlation using the coupled electron pair approximation. This polarizability is found to be further diminished to around 400 au on introducing a realistic model of the full environment in the cryptand. The electron correlation contribution to the polarizability is largely suppressed on entering the condensed phase. The diamagnetic contribution to the susceptibility is found to be reduced in magnitude by 32% on introducing a model for the full environment in the cryptand. This result, combined with an average energy approximation analysis of the ab-initio polarizabilities, shows that environmental modifications of the ground-state wave functions are responsible for about one-third of the polarizability reductions, with two-thirds arising from environmental modifications of the excited states and their excitation energies. The contribution of the two 3s electrons to the diamagnetic part of the nuclear shielding is found to be enhanced by 9% when the free anion experiences the present model for the environment in the cryptand, the core contribution remaining essentially unchanged. The nucleus in the cryptated anion is predicted to be shielded by 3.58 ppm relative to that in an isolated gaseous sodium atom, compared with the 2.88 ppm nuclear shielding in the free anion relative to that in the free atom. This comparative insensitivity of the shielding is consistent with the experimental observation that the Na^- shielding (uncorrected for bulk susceptibility) almost always lies within ±1 ppm of a 1.5 ppm shielding relative to the free sodium atom. This explains how the nuclear shielding can be so comparatively environment insensitive in a species interacting sufficiently strongly with its surroundings as to experience a reduction in polarizability by a factor of 2.7.

I. Introduction

The singly charged anion of an alkali metal is described, in the orbital model of the electronic structure of an atom, as containing two spin-paired electrons in its *n*s valence orbital, thus having the configuration ns^2. The anions of all the alkali metals have been prepared in the gas phase and their ionization potentials measured by photodetachment.[1] The result that an energy in the range of 0.5 eV is required to ionize any alkali metal anion (M^-) to produce the neutral atom (M) shows that these anions exist as stable species in the gas phase, having infinite lifetimes if left unperturbed. In 1953, many years before these experiments, it was suggested[2] that alkali anions might also exist in the condensed phase. Roughly contemporaneously with the photodetachment measurements, this possibility was unambiguously realized by Dye and co-workers. They both identified the sodium anion (Na^-) in solutions prepared by dissolving sodium metal in a mixture of ethylamine and a cryptand[3] as well as synthesized a crystalline salt containing Na^- ions whose structure was determined by X-ray crystallography.[4,5] The sodium anion has subsequently been identified in a wide range of solutions produced by dissolving sodium in other solvents containing added cryptands as well as in solutions of sodium in amines or crown ethers. The anions of K, Rb, and Cs were subsequently identified in solutions prepared by dissolving the appropriate metal in such solvents. Furthermore, the structures of several salts containing either the Rb^- or the Cs^- ion have been determined by X-ray crystallography. Any of three reviews[6–8] of this work contain references to the original literature.

Solutions containing alkali anions have been studied using a variety of techniques such as pulse radiolysis[9] and ultraviolet,[10] EPR,[11] and NMR[6–8] spectroscopy, of which the latter has been used most widely. The frequency of the nuclear resonance signal originating from the sodium anion is found not only to be almost independent of both temperature and concentration but also to be independent of solvent. Furthermore, this signal occurs at almost the same frequency in the crystalline salts containing Na^- as it does in solution. Each of these NMR experiments yields the shielding of the nucleus in Na^- relative to that of the ^{23}Na nucleus in hydrated sodium cations at infinite dilution. These

---

[†] University Chemical Laboratory, Cambridge.

[‡] University of Birmingham.

(1) Patterson, T. A.; Hotop, H.; Kashdan, A.; Norcross, D. W.; Lineberger, W. C. *Phys. Rev. Lett.* **1974**, *32*, 189.

(2) Bingel, W. *Ann. Phys.* (*Leipzig*) **1953**, *12*, 57.

(3) Ceraso, J. M.; Dye, J. L. *J. Chem. Phys.* **1974**, *61*, 1585.

(4) Dye, J. L.; Ceraso, J. M.; Lok, M. T.; Barnett, B. L.; Tehan, F. J. *J. Am. Chem. Soc.* **1974**, *96*, 608.

(5) Tehan, F. J.; Barnett, B. L.; Dye, J. L. *J. Am. Chem. Soc.* **1974**, *96*, 7203.

(6) Edwards, P. P. *Adv. Inorg. Chem. Radiochem.* **1982**, *25*, 135.

(7) Dye, J. L. *Prog. Inorg. Chem.* **1984**, *32*, 327.

(8) Edwards, P. P.; Ellaboudy, A.; Holton, D. M.; Pyper, N. C. *Annu. Rep. NMR Spectrosc.* **1988**, *20*, 315.

(9) Fletcher, J. W.; Seddon, W. A. *J. Phys. Chem.* **1975**, *79*, 3055.

(10) Dye, J. L. *Angew. Chem., Int. Ed. Engl.* **1979**, *18*, 587.

(11) Catterall, R. *Metal Ammonia Solutions*; Lagowski, J. J., Sienko, M. J., Eds.; Butterworths: London, 1970; p 105.

0002-7863/93/1515-1468$04.00/0